

# The Properties of Intergalactic CIV Absorption II: Which Systems Are Associated With Galaxy Outflows?

Antoinette Songaila<sup>1</sup>

*Institute for Astronomy, University of Hawaii, 2680 Woodlawn Drive, Honolulu, HI 96822*

acowie@ifa.hawaii.edu

## ABSTRACT

Using the extremely high S/N quasar absorption-line sample described in the first paper of the series, we investigate which intergalactic C IV absorption line systems could be directly associated with galactic outflows at  $z = 2 - 3.5$  from an analysis of the velocity widths of the C IV absorption line systems. Only about half the systems with a peak  $\tau(\text{CIV})$  above 0.4 in the  $\lambda 1548 \text{ \AA}$  line (roughly a column density of C IV above about  $2 \times 10^{13} \text{ cm}^{-2}$ ) have velocity widths large enough to originate in this way, and very few of the weaker systems do. The median velocity full width at a tenth max is found to be  $50 \text{ km s}^{-1}$  for systems with peak  $\tau(\text{CIV})$  in the range 0.1–0.4 and  $160 \text{ km s}^{-1}$  for systems with a peak  $\tau(\text{CIV})$  in the range 0.4–3. We show that this critical value of  $\tau(\text{CIV})$  also separates systems that could be ionized by galaxy-like spectra from those in which the ionization is clearly AGN-dominated. Together the results are consistent with a picture in which almost all the lower column density, and at least half the higher column density, systems lie in the more general IGM whereas about half of the higher column density systems could be produced directly by the outflows and possibly be ionized by their parent galaxies.

*Subject headings:* cosmology: observations — early universe — quasars: absorption lines — galaxies: evolution — galaxies: formation

## 1. Introduction

It is well known that C IV enrichment appears to be a ubiquitous feature of the intergalactic Ly $\alpha$  forest at least down to  $\tau(\text{Ly}\alpha)$  approaching 1 (Cowie et al. 1995; Tytler et

---

<sup>1</sup>Visiting Astronomer, W. M. Keck Observatory, which is jointly operated by the California Institute of Technology, the University of California, and the National Aeronautics and Space Administration

al. 1995; Songaila & Cowie 1996; Songaila 1998; Ellison et al. 2000; Songaila 2001; Aguirre, Schaye & Theuns 2002; Schaye et al. 2003; Simcoe, Sargent & Rauch 2004; Aguirre et al. 2004) and possibly even at lower values (Cowie & Songaila 1998; Ellison et al. 2000; Aguirre, Schaye & Theuns 2002), albeit with substantial variation (of about a dex) in individual C IV/H I ratios at every overdensity and with an equally significant trend with overdensity (Schaye et al. 2003). The origin of these metals is still unclear: some may be being injected into the IGM from galaxies at the redshifts in question (Steidel, Pettini & Adelberger 2001; Adelberger et al. 2003; Adelberger et al. 2005) while others may have been put in place by earlier galaxy formation or by generations of population III stars (Gnedin & Ostriker 1997; Cen & Ostriker 1999; Wasserburg & Qian 2000; Madau, Ferrara & Rees 2001; Qian, Sargent & Wasserburg 2002; Bromm, Yoshida & Hernquist 2003; Venkatesan & Truran 2003; Mackey, Bromm & Hernquist 2003; Fujita et al. 2004; Daigne et al. 2004; Yoshida, Bromm & Hernquist 2004).

This issue of the fraction arising from current injection versus that from early star formation has been brought into prominence by two sets of observations. The first is the invariance of the column density distribution and the total  $\Omega(\text{CIV})$  as a function of redshift which we have discussed in Paper I (Songaila 2005; see also Songaila 1997, 2001; Pettini et al. 2003; Schaye et al. 2003). These observations show directly that a substantial amount of metals was in place prior to  $z = 5$  and also that subsequent injection processes and changes in the ionization environment have not greatly changed the total amount of C IV or the way it is distributed in column density. The second is the observation by Adelberger and collaborators that there is a strong correlation between the C IV absorbers and the Lyman break galaxies (LBGs) at redshifts near 3 which they argue suggests that some part of the C IV absorption may arise, at least in part, from the outflows from these galaxies (Steidel, Pettini & Adelberger 2001; Adelberger et al. 2003; Adelberger et al. 2005). However, Porciani & Madau (2005) show that this correlation can be present even if the metals are injected from early ( $z = 6 - 12$ ) small galaxies. In this interpretation the correlation arises because both galaxies and the intergalactic absorption lines are biased to overdense regions. There is also still substantial statistical uncertainty in the galaxy-C IV correlation function (Adelberger et al. 2005).

Higher column density systems, including those associated with damped Ly $\alpha$  systems, have long been believed to lie in the extended disks or halos of galaxies. Indeed, Adelberger et al. 2005 find that roughly a third of C IV absorbers with  $N(\text{C IV}) > 10^{14} \text{ cm}^{-2}$  are directly associated with LBGs at  $z = 2$ . However, the lower column density C IV systems have been modelled as originating in the more distributed IGM. Viewed in this way the results discussed above are less incongruous and the question may instead be posed as: above what column density does gas associated with individual galaxies constitute a major part of the C IV

absorption line population? It is this question we shall attempt to answer in the present paper by looking at the internal properties of the C IV absorption line systems, and, in particular, their velocity and ionization structure.

We show that the velocity and ionization properties in combination suggest that there is a transition at a critical column density of  $N(\text{CIV}) \sim 2 \times 10^{13} \text{ cm}^{-2}$ . Below this column density most of the absorbers are not currently being ejected by the galaxies but above this the fraction of the absorbers that could be arising in galactic outflows increases. If, as this suggests, a substantial fraction of the C IV absorbing material is generated in earlier star formation, it becomes easier to understand the invariance of C IV with redshift. However, the maintenance of the shape of the distribution function in the redshift range  $z = 1.5 - 5$  is still surprising in view of the multiple mechanisms that are probably responsible for creating and ionizing the absorption lines.

We first reprise some simple numerical arguments to motivate our analysis. Throughout we use a cosmology with  $H_0 = 65 \text{ km s}^{-1} \text{ Mpc}^{-1}$ ,  $\Lambda = 0.67$  and  $\Omega = 0.33$ .

In order to occupy sufficient volume to produce the C IV absorption lines seen in the intergalactic medium the metals streaming from the galaxies must have a very high terminal velocity. The number of absorption line systems with column densities greater than  $N$  per unit absorption length  $dX$  is given by

$$n(> N) = \frac{c}{H_0} \sigma n_0 \quad (1)$$

where  $\sigma$  is the fixed cross section of the bubble of C IV absorbing material around each galaxy,  $n_0$  is the comoving number density of the galaxies (e.g. Burbidge et al. 1977) and  $dX$  is defined as

$$dX = \frac{(1+z)^2 dz}{[(1+z)^2(1+\Omega_m z) - z(z+2)\Omega_\lambda]^{0.5}} \quad (2)$$

For the adopted cosmology the total observed comoving number density of LBGs above an R magnitude of 27 at  $z = 3$  is  $\approx 5 \times 10^{-3} \text{ Mpc}^{-3}$  (Adelberger & Steidel 2000). Since  $n(> N)$  is 3.1 for  $N = 10^{13} \text{ cm}^{-2}$  at these redshifts we would require a cross sectional radius of about 200 kpc per LBG to account for the observed absorption systems above this column density. Then, since the age of the universe is approximately 1 Gyr at this redshift, we must have a minimum expansion velocity of over  $200 \text{ km s}^{-1}$  in the material producing the C IV absorbers. Clustering, partial covering in the bubble of expanding material, or shorter lifetimes would all increase the required velocity. It is the coincidence of this required terminal velocity with the observed expansion velocities in the LBGs that has motivated the idea that the C IV systems could arise in this way.

The above discussion assumes that every line of sight through the bubble samples C IV absorbing material, which appears plausible if there is considerable entrained material in the wind. If the bubbles were patchy the radius would have to be larger to give the same cross section, which would begin to stretch the required velocity relative to that seen in the LBGs. However, if the C IV is ubiquitous in the bubble we will see it over the line-of-sight velocity range of the projected line-of-sight through the bubble. For a spherical geometry the average line width will then be 1.3 times the terminal velocity, and over most of the face of the bubble the line width will be close to this value.

Therefore it appears that C IV absorption lines arising in the galaxy outflows should show large velocity widths of about 300-400 km s<sup>-1</sup>. Galaxies with lower outflow velocities would have too small a cross section to produce significant C IV absorption along a typical line of sight. Furthermore, since there are more low column density C IV systems, the characteristic velocity width would have to rise with decreasing column density for the number of weaker systems to be understood.

Since the bubble absorbers lie close to their host galaxies they may also experience a proximity effect in which the dominant ionization field becomes that of the galaxy rather than the metagalactic flux. At low redshift the metagalactic flux may be AGN-dominated, which would distinguish it from the galaxy spectral shape. The line ratios of Si IV/C IV versus those of C II/C IV are very different for the two cases and in the second part of the paper we briefly investigate this alternate diagnostic.

## 2. Velocity structure

Motivated by the above discussion we first examine the velocity widths of the C IV absorption systems to determine which systems are wide enough to be understood as galaxy outflows and to determine if there is any dependence of the velocity width on the column density of the C IV absorbers.

For this analysis we use the cleaned  $\tau(\text{CIV})1548$ , defined in paper I, which is the measured  $\tau(\text{CIV})1548$  at all positions where the C IV doublet ratio is approximately consistent with the expected value ( $\tau(\text{CIV})1548/\tau(\text{CIV})1550$  between 1 and 4) and zero otherwise. We used the core sample of five ultra-high S/N quasars described in Paper I: Q0636+680 ( $z_{\text{em}} = 3.18$ , S/N = 220), HS0741+4741 ( $z_{\text{em}} = 3.22$ , S/N = 210), Q1422+2309 ( $z_{\text{em}} = 3.62$ , S/N = 340), HS1700+6416 ( $z_{\text{em}} = 2.72$ , S/N = 205), HS1946+7658 ( $z_{\text{em}} = 3.03$ , S/N = 210).

In making this analysis we need to characterise the absorption system with a parameter that is not dependent on the velocity structure of the system. In particular, high column density systems may be preferentially selected to be wide in velocity space. We have chosen, therefore, to measure the strength of the system by using the largest optical depth in the C IV 1548 line, which we refer to as the peak optical depth,  $\tau_p$ . In fact  $\tau_p$  is tightly related to  $N(\text{CIV})$  determined from Voigt profile fitting, as we show in Figure 1. The ratio  $N(\text{CIV})/\tau_p$  is proportional to the velocity integral of  $\tau$  divided by the peak optical depth and so measures the optical depth-weighted velocity spread in the system (i.e. the total velocity width over which the bulk of the material arises). Empirically, the column density is related to the peak  $\tau_p$  as

$$N(\text{CIV}) = 5.4 \times 10^{13} \tau_p^{1.11} \text{ cm}^{-2} \quad , \quad (3)$$

meaning that the higher column density absorbers are systematically wider than the lower column density ones, though the rise is not rapid. Nearly all the absorbers fall within a multiplicative factor of two of this relation so the dispersion of the optical-depth-weighted velocity widths at any given  $\tau_p$  is not large.

For the present analysis we want a quantity that is a measure of the full spread in velocity of each system and that is not a function of the strength of the system. We choose to define the width of the system as the maximum difference in velocity between positions in the system that satisfy the condition that  $\tau$  is greater than some fraction of the peak  $\tau$ . This definition does not require that there be continuous absorption above this value throughout the velocity range and therefore we must restrict the search to some finite velocity range. We choose to search to positions that lie within  $350 \text{ km s}^{-1}$  of the peak  $\tau$ , which in turn restricts the maximum measurable width to a value of  $700 \text{ km s}^{-1}$ . This is appropriate if we want to look at the velocity spread of patchy material spread throughout an outflow. The procedure will occasionally connect neighboring absorption line systems which are not in fact causally connected. This will then result in a large overestimate of the velocity width for the occasional individual system. Such contamination is more probable at lower  $\tau$  where there is a higher density of systems and must be dealt with statistically by modelling the number of chance connections that occur.

For each of the 5 quasars we searched a region of the spectrum longward of the quasar’s  $\text{Ly}\alpha$ , and also more than  $10,000 \text{ km s}^{-1}$  shortward of the quasar’s C IV emission to avoid forest contamination and C IV systems associated with the quasar itself. We worked downward in optical depth to select the systems, restricting ourselves to  $\tau_p$ s that were more than two velocity windows from an existing system. The final sample contains 53 C IV absorption line systems with a range of  $\tau_p$  from 0.1 to 4. The systems range in redshift from 2.0 to 3.6 with a median of 2.7. Information on the 53 systems is collected in Table 1 which lists index number, quasar, redshift and value of the automatically-determined peak optical depth

within the system, full width at tenth max (FWTM), and Voigt profile-fitted values of the system’s centroid redshift and C IV, Si IV and C II column densities. The 53 systems are shown in Figures 2 to 4.

In order to choose an appropriate cut value for the ratio of the optical depth to the peak optical depth at which to measure the velocity width, we analysed the growth in width versus cut value for the stronger absorption line systems in the sample ( $1.4 < \tau_p < 3$ ). This is shown in Figure 5. The measured velocity widths approach the asymptotic values as the cut level is reduced, and the average width has reached 85% of the asymptotic value at a cut of 0.1. We adopt this value for the analysis, referring to this as the full width at tenth max (FWTM) of the absorption system. Cutting at such a low level places stringent demands on the S/N of the quasar sample and, even for the very high S/N data of the present quasar sample, restricts us to absorption systems with  $\tau_p$  in excess of 0.1.

Samples of the FWTM measure of absorption line systems with a wide range in  $\tau_p$  are shown in Figure 6 where we also show the corresponding CII and Ly $\alpha$  lines for comparison. In each case the thick solid line shows the measured width of the system. In nearly all cases the measured velocity spread lies within the saturated portions of the corresponding L $\alpha$  line, and where CII absorption is seen it is generally comparable to or narrower than the velocity spread seen in the C IV line. A probable example of a case where the method has actually joined two independent systems is shown in Figure 7, though in any given case we can only statistically estimate how likely such a chance projection is.

The measured velocity widths for the systems are shown as a function of  $\tau_p$  in Figure 8 and the corresponding histograms of the distributions in two  $\tau_p$  ranges are shown in red in Figure 9. In order to estimate the degree of contamination we adopted a procedure in which the redshift positions of the  $\tau_p$ s were inserted into the spectrum of one of the other quasars and the FWTM measured around this position using the same procedure as in the real systems. In most cases this is zero but contamination results in a number of systems in which a non-zero width is measured. The advantage of this procedure over simulations is that it properly includes the effects of systematics in the spectra, such as incompletely subtracted sky lines, telluric absorption, poor continuum fitting, etc. The process produces a false sample which is slightly less than four times the true sample (since only overlapping portions of the spectra can be used) and which can be scaled to estimate the number of contaminating systems in the true sample. The expected contamination is shown by the green histograms of Figure 9.

At low  $\tau_p$  almost all of the wide systems (FWTM  $> 150$  km s $^{-1}$ ) are false. Seven systems are observed, whereas the analysis of the false sample predicts that there should be 8.7 systems with random widths of this value. The  $1 \sigma$  upper limit on the number of real

systems is 2. At widths less than  $150 \text{ km s}^{-1}$  there are 26 systems and we expect 4.9 systems. Therefore, fewer than 10% of the weak C IV absorbers are wide. The median width of the distribution corrected for the false cases is  $50 \text{ km s}^{-1}$  and the systems are closely distributed around this value. In contrast, contamination is, as expected, a much less serious problem at high  $\tau_p$  and here there is a much wider spread in the FWTM velocity width and even a suggestion of bimodality, though the number of systems is too small for this to be highly significant. The median value is  $160 \text{ km s}^{-1}$  and the maximum velocity width is about  $300 \text{ km s}^{-1}$ .

We conclude that at low  $\tau_p$  ( $< 0.4$ ) the systems are too narrow to be plausibly associated with galaxy outflows but that at higher  $\tau_p$  some systems are much wider and it is possible that at least some fraction of the systems are formed in this way. The dividing  $\tau_p$  of about 0.4 corresponds to a column density  $N(\text{CIV})$  of  $2 \times 10^{13} \text{ cm}^{-2}$ . We emphasize that the data are of sufficiently high quality that such systems could be detected easily.

### 3. Ionization balance

A luminous Lyman break galaxy at  $z = 3$  with an observed  $AB$  magnitude of about 24 at the redshifted Lyman continuum would produce an outgoing ionizing flux of about  $4 \times 10^{-22} (\phi/0.01) (R/200 \text{ kpc}) \text{ erg cm}^{-2} \text{ s}^{-1} \text{ Hz}^{-1}$  just below the ionization edge. Here  $\phi$  is the escape fraction of ionizing photons and  $R$  is the radial separation of the absorber from the galaxy. Within the considerable uncertainty in the escape fraction (e.g. Steidel, Pettini & Adleberger 2001; Giallongo et al. 2002) the ionization of associated absorbers could be dominated by the galaxy or, if the escape fraction is low, by the average metagalactic flux. Thus it is possible that we might be able to distinguish between absorbers in galaxy outflows and those in the general IGM based on their ionization balance.

The simplest test is to consider the ratio Si IV/C IV ion versus C II/C IV. As is well known (e.g. Rauch, Haehnelt, & Steinmetz 1997) galactic spectra that cut off at high energies produce high Si IV/C IV ratios even in systems with high ionization parameters and low C II/C IV. In contrast, with an AGN power law spectrum Si IV/C IV drops as C II/C IV does.

The various ions may have somewhat different velocity structure; in particular, C II is often different from C IV. For this reason, we use in this section the Voigt profile-fitted column densities given in Table 1, which are fitted over the whole range of visible components, and, for consistency, the FWTM velocity width measured on the Voigt profile fit. We show the comparison of the two FWTM velocities in Figure 10. In general, the two measures

agree extremely well except for the small number of cases where the Voigt fitting has split a system treated as one complex by the automatic procedure into two complexes.

In Figure 11 we show the ratios for the 18 systems in Table 1 where both C II and Si IV lie above the Lyman alpha forest and where the redshift of the absorber is less than 3.1 (chosen to roughly lie at the upper boundary of He II reionization). Systems with high velocity spreads based on the Voigt fitted FWTM are shown by filled squares while those with  $dv(\text{FWTM}) < 100 \text{ km s}^{-1}$  are shown with open diamonds. All of the systems are roughly consistent with a simple AGN ionization model with a Si/C abundance of 2.5 times solar, shown by the solid line. Nearly all of the narrow systems have Si IV/C IV values that are well below that expected from a galaxy ionizing spectrum even with a solar Si/C abundance. We can conclude therefore that the narrow systems are ionized by an AGN-dominated metagalactic flux. The broader systems, which generally have higher column densities, have lower ionization parameters and higher ratios, mostly lie in the region where the differentiation is less clear, and, particularly in view of possible flexibility in the Si/C abundance, could be ionized by either a galaxy spectrum or an AGN one.

In Figure 12 we show the dependence of C II/C IV and Si IV/C IV as a function of  $\tau_p$  and of  $dv(\text{FWTM})$ . C II/C IV shows an almost linear relation with  $\tau_p$  (though with some spread) reflecting the fact that higher column density absorbers have lower ionization parameters (e.g. Shaye et al. 2003). Si IV/C IV shows a shallower but smooth rise with  $\tau_p$ . The near linearity of C II/C IV is a fairly natural consequence of a model in which the absorbers arise in the general IGM since C II/C IV is roughly dependent on the inverse of the ionization parameter or, for a fixed ionization, the absorber density, whereas the C IV column density (or  $\tau_p$ ) is a rough measure of the absorber column density which in turn roughly follows the overdensity of the system. However, this uniformity of behaviour would be much harder to understand in a model in which the bulk of the absorbers arose in a galactic outflow and where individual absorber properties might be expected to depend on the strength of the outflow, the hydrodynamic convection and fragmentation, and the properties of the galaxy itself, as well as any galaxy contribution to the ionization.

The C II/C IV ratio plotted versus velocity width does show a suggestion of a transition at  $dv = 100 \text{ km s}^{-1}$ : systems with lower velocity spreads are almost invariably high-ionization systems with low C II/C IV whereas the wide systems show much more of a range in C II/C IV values. Consistent with the velocity analysis, this might suggest that wide velocity systems could comprise a mixture of galaxy outflow and IGM systems. However, the number of systems is too small for the abruptness of the transition to be a robust conclusion and the data could be consistent with a smooth evolution of C II/C IV with  $dv$ , where this would be a simple corollary of the density dependence discussed in the previous paragraph.



#### 4. Conclusions

The primary result of this paper is that weak C IV absorption systems ( $\tau_p < 0.4$  or  $N(\text{C IV}) < 2 \times 10^{13} \text{ cm}^{-2}$ ) almost all lie in narrow complexes with a median FWTM of  $50 \text{ km s}^{-1}$ . It appears that these systems cannot be easily understood in terms of high-velocity galactic-wind outflows from galaxies that are active at that time. Because there are so few wide systems in the low- $\tau_p$  sample (fewer than 10%), the covering factor would have to be much less than 1 and the bubble size and outflow velocity unreasonably large when compared with observations of Lyman break galaxies. These systems also appear to be ionized by an AGN-like spectrum. As many as half of the stronger C IV systems are wide enough that they could be produced in local outflows and in some cases could be ionized primarily by the parent galaxy, so that as many as half of higher column density systems could be associated with contemporary outflows from galaxies.

This research was supported by the National Science Foundation under grant AST 00-98480.

#### REFERENCES

- Adelberger, K. L., & Steidel, C. C. 2000, *ApJ*, 544, 218
- Adelberger, K. L., Steidel, C. C., Shapley, A. E., & Pettini, M. 2003, *ApJ*, 584, 45
- Adelberger, K. L., Shapley, A. E., Steidel, C. C., Pettini, M., Erb, D. K., & Reddy, N. A. 2005, *ApJ*, in press (astro-ph/0505122)
- Aguirre, A., Schaye, J. & Theuns, T. 2002, *ApJ*, 576, 1
- Aguirre, A., Schaye, J., Kim, T.-S., Theuns, T., Rauch, M. & Sargent, W. L. W. 2004, *ApJ*, 602, 38
- Bromm, V., Yoshida, N., & Hernquist, L. 2003, *ApJL*, 596, L135
- Burbidge, G., Odell, S. L., Roberts, D. H., & Smith, H. E. 1977, *ApJ*, 218, 33
- Cen, R. & Ostriker, J. P. 1999, *ApJ*, 519, L109
- Cowie, L. L., Songaila, A., Kim, T.-S., & Hu, E. M. 1995, *AJ*, 109, 1522
- Cowie, L. L., & Songaila, A. 1998, *Nature*, 394, 44
- Daigne, F., Olive, K. A., Vangioni-Flam, E., Silk, J., & Audouze, J. 2004, *ApJ*, 617, 693
- Ellison, S. L., Songaila, A., Schaye, J. & Pettini, M. 2000, *AJ*, 120, 1175

- Fujita, A., Mac Low, M.-M., Ferrara, A., & Meiksin, A. 2004, ApJ, 613, 159
- Giallongo, E., Cristiani, S., D’Odorico, S., & Fontana, A., 2002, ApJ 568, L9
- Gnedin, N. Y. & Ostriker, J. P. 1997, ApJ, 486, 581
- Madau, P., Ferrar, A., & Rees, M. J. 2001, ApJ, 555, 92
- Mackey, J., Bromm, V., & Hernquist, L. 2003, ApJ, 586, 1
- Pettini, M., Madau, P., Bolte, M., Prochaska, J. X., Ellison, S. L., & Fan, X. 2003, ApJ, 594, 695
- Porciani, C., & Madau, P. 2005, ApJ, 625, L43
- Qian, Y.-Z., Sargent, W. L. W., & Wasserburg. G. J. 2002, ApJL, 569, L61
- Rauch, M., Haehnelt, M. G., & Steinmetz, M. 1997, ApJ, 481, 601
- Schaye, J., Aguirre, A., Kim, T.-S., Theuns, T., Rauch, M. & Sargent, W. L. W. 2003, ApJ, 596, 768
- Simcoe, R. A., Sargent, W. L. W., & Rauch, M. 2004, ApJ, 606, 92
- Songaila, A. 1997, ApJ, 490, L1
- Songaila, A. 1998, AJ, 115, 2184
- Songaila, A. 2001, ApJ, 561, L153
- Songaila, A. 2005, AJ, in press (Nov. 2005) (astro-ph/0507649; Paper I)
- Songaila, A. & Cowie, L. L. 1996, AJ, 112, 335
- Steidel, C. C., Pettini, M. & Adelberger, K. L. 2001, ApJ, 546, 665
- Tytler, D., et al. 1995, in QSO Absorption Lines, ESO Astrophysics Symposia, ed. G. Meylan (springer, Heidelberg), p. 289
- Venkatesan, A., & Truran, J. 2003, ApJL, 594, L1
- Wasserburg, G. J., & Qian, Y.-Z. 2000, ApJL, 538, L99
- Yoshida, N., Bromm, V., & Hernquist, L. 2004, ApJ, 605, 579

Table 1. The C IV Sample

Number	Quasar	$z_{peak}$	$\tau_{peak}$	$dv$	$z_{cen}$	$N_{CIV}$	$N_{SiIV}$	$N_{CII}$
1	HS1700+6416	2.31484	4.00	183	2.31536	1.9e+15	6.1e+13	0.0e+00
2	Q0636+680	2.47528	3.25	244	2.47416	1.7e+14	0.0e+00	0.0e+00
3	Q0636+680	2.90459	2.86	212	2.90374	3.0e+14	1.4e+14	1.2e+14
4	HS1700+6416	2.16793	2.66	42	2.16795	1.0e+14	1.7e+13	1.3e+13
5	HS0741+4741	2.58354	1.88	99	2.58334	1.0e+14	0.0e+00	0.0e+00
6	HS0741+4741	2.69237	1.61	245	2.69235	6.5e+13	3.7e+12	0.0e+00
7	Q1422+2309	3.53865	1.56	272	3.53863	1.8e+14	3.7e+13	4.0e+13
8	HS0741+4741	2.73297	1.43	121	2.73323	4.8e+13	4.3e+12	1.9e+13
9	Q0636+680	3.01724	1.27	317	3.01749	4.1e+13	1.1e+12	7.0e+11
10	HS0741+4741	2.64916	1.07	63	2.64921	5.3e+13	5.2e+12	0.0e+00
11	Q1422+2309	2.74886	1.00	113	2.74891	4.1e+13	0.0e+00	0.0e+00
12	HS1946+7658	2.64432	1.00	23	2.64437	2.3e+13	3.7e+11	0.0e+00
13	HS0741+4741	3.01778	0.85	117	3.01763	8.4e+13	2.4e+13	1.6e+15
14	Q0636+680	2.31119	0.63	157	2.31098	7.2e+13	0.0e+00	0.0e+00
15	Q1422+2309	3.38159	0.61	204	3.38277	4.8e+13	3.1e+12	1.1e+12
16	HS1700+6416	2.43869	0.58	280	2.43863	5.2e+13	3.4e+12	1.3e+12
17	Q0636+680	2.89183	0.52	215	2.89163	3.0e+13	-1.7e+11	4.5e+09
18	Q1422+2309	3.08354	0.50	245	3.08354	4.1e+11	0.0e+00	0.0e+00
19	HS1700+6416	2.57802	0.49	110	2.57857	3.6e+13	1.3e+12	1.9e+12
20	HS1700+6416	2.37988	0.44	31	2.37984	1.2e+13	1.1e+12	0.0e+00
21	Q1422+2309	2.96195	0.39	155	2.96228	3.4e+13	0.0e+00	0.0e+00
22	HS0741+4741	2.67287	0.37	107	2.67283	1.8e+13	-5.7e+11	0.0e+00
23	HS0741+4741	3.06665	0.35	59	3.06656	2.0e+13	3.1e+11	3.3e+11
24	Q1422+2309	2.69835	0.33	221	2.69795	3.1e+13	0.0e+00	0.0e+00
25	HS0741+4741	2.90527	0.31	232	2.90455	2.4e+13	7.8e+11	2.2e+12
26	HS1946+7658	2.89309	0.31	101	2.89271	2.5e+13	4.9e+12	2.9e+12

Table 1—Continued

Number	Quasar	$z_{peak}$	$\tau_{peak}$	$dv$	$z_{cen}$	$N_{CIV}$	$N_{SiIV}$	$N_{CII}$
27	Q1422+2309	3.51459	0.30	44	3.51473	1.0e+13	1.4e+12	-3.3e+11
28	Q1422+2309	2.89538	0.29	69	2.89509	1.3e+13	0.0e+00	0.0e+00
29	HS0741+4741	2.62110	0.28	112	2.62123	1.7e+13	3.8e+11	0.0e+00
30	Q1422+2309	3.13440	0.25	357	3.13413	1.6e+13	1.1e+12	0.0e+00
31	HS1946+7658	2.39519	0.25	25	2.39528	5.7e+12	0.0e+00	0.0e+00
32	HS0741+4741	3.05360	0.23	19	3.05366	8.1e+12	1.3e+13	-2.8e+11
33	Q1422+2309	2.97619	0.23	366	2.97621	8.1e+12	0.0e+00	0.0e+00
34	Q0636+680	2.86874	0.23	92	2.86883	6.4e+12	2.9e+10	-3.9e+11
35	HS1700+6416	2.02108	0.22	35	2.02108	8.3e+12	2.4e+11	0.0e+00
36	Q0636+680	2.32485	0.22	52	2.32492	9.3e+12	0.0e+00	0.0e+00
37	Q1422+2309	2.68275	0.22	49	2.68257	7.1e+12	0.0e+00	0.0e+00
38	HS1700+6416	2.28955	0.20	49	2.28952	6.8e+12	6.2e+10	0.0e+00
39	HS1946+7658	2.77725	0.20	35	2.77731	4.9e+12	-1.3e+11	-4.7e+11
40	Q0636+680	2.68207	0.19	204	2.68228	9.6e+12	-1.5e+11	0.0e+00
41	HS1700+6416	2.56826	0.19	45	2.56817	6.6e+12	2.6e+11	-5.5e+10
42	HS1700+6416	2.19884	0.19	54	2.19893	6.7e+12	5.2e+10	0.0e+00
43	Q1422+2309	2.72015	0.19	33	2.72009	6.1e+12	0.0e+00	0.0e+00
44	HS1700+6416	2.12775	0.17	30	2.12778	6.1e+12	-3.3e+11	0.0e+00
45	HS0741+4741	2.96511	0.16	94	2.96530	8.5e+12	-4.4e+11	2.6e+11
46	HS1946+7658	2.91663	0.16	49	2.91661	5.4e+12	-1.6e+11	6.7e+10
47	Q1422+2309	3.41150	0.15	78	3.41121	9.3e+12	1.5e+12	1.3e+12
48	Q1422+2309	2.94748	0.13	330	2.94754	3.0e+12	0.0e+00	0.0e+00
49	HS1946+7658	2.65414	0.13	66	2.65424	7.8e+12	1.5e+11	0.0e+00
50	HS0741+4741	3.03513	0.13	93	3.03469	1.0e+13	9.7e+11	5.9e+10
51	HS0741+4741	2.71463	0.12	46	2.71446	6.3e+12	2.8e+11	0.0e+00
52	Q0636+680	2.62142	0.11	58	2.62115	6.7e+12	0.0e+00	0.0e+00

Table 1—Continued

Number	Quasar	$z_{peak}$	$\tau_{peak}$	$dv$	$z_{cen}$	$N_{CIV}$	$N_{SiIV}$	$N_{CII}$
53	Q1422+2309	2.99918	0.11	28	2.99922	4.7e+12	0.0e+00	0.0e+00

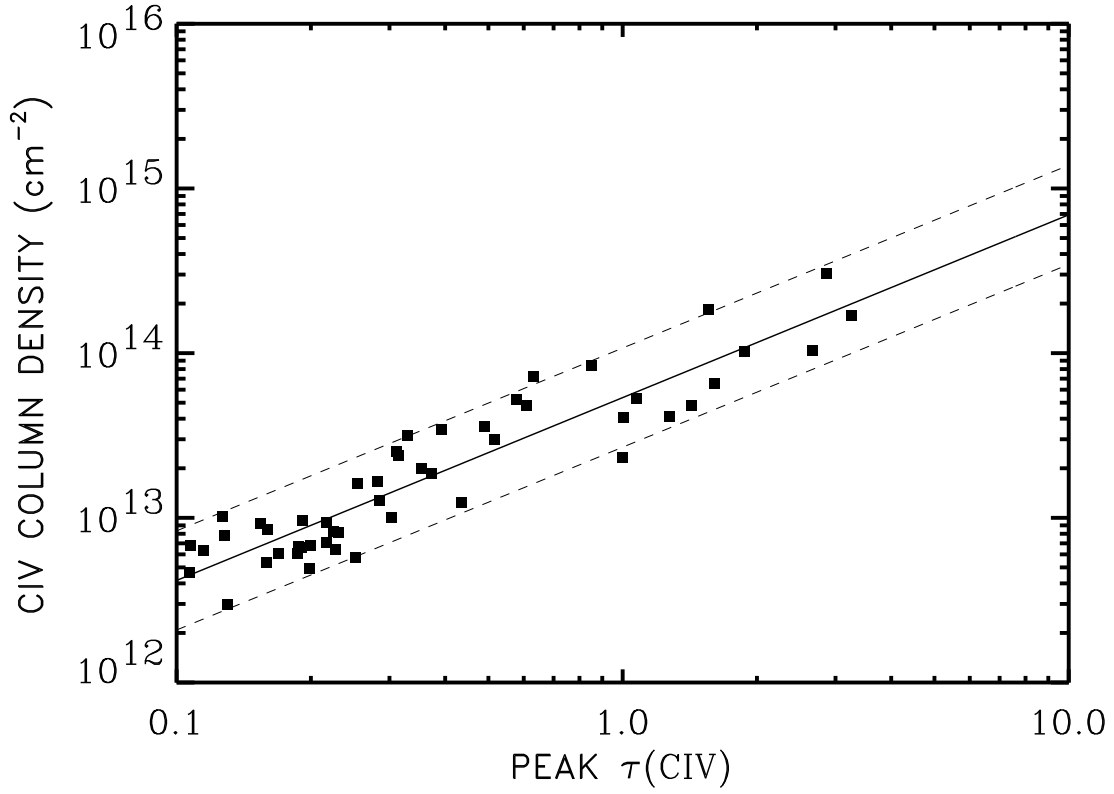


Fig. 1.— *Filled squares* : C IV column density determined from Voigt profile fitting versus the peak optical depth of the C IV 1548 line in the system. *Solid line* : the power law fit  $N(\text{CIV}) = 5.4 \times 10^{13} \tau(\text{CIV})^{1.11} \text{ cm}^{-2}$ . *Dashed lines* : a multiplicative range of 2 about this fit.

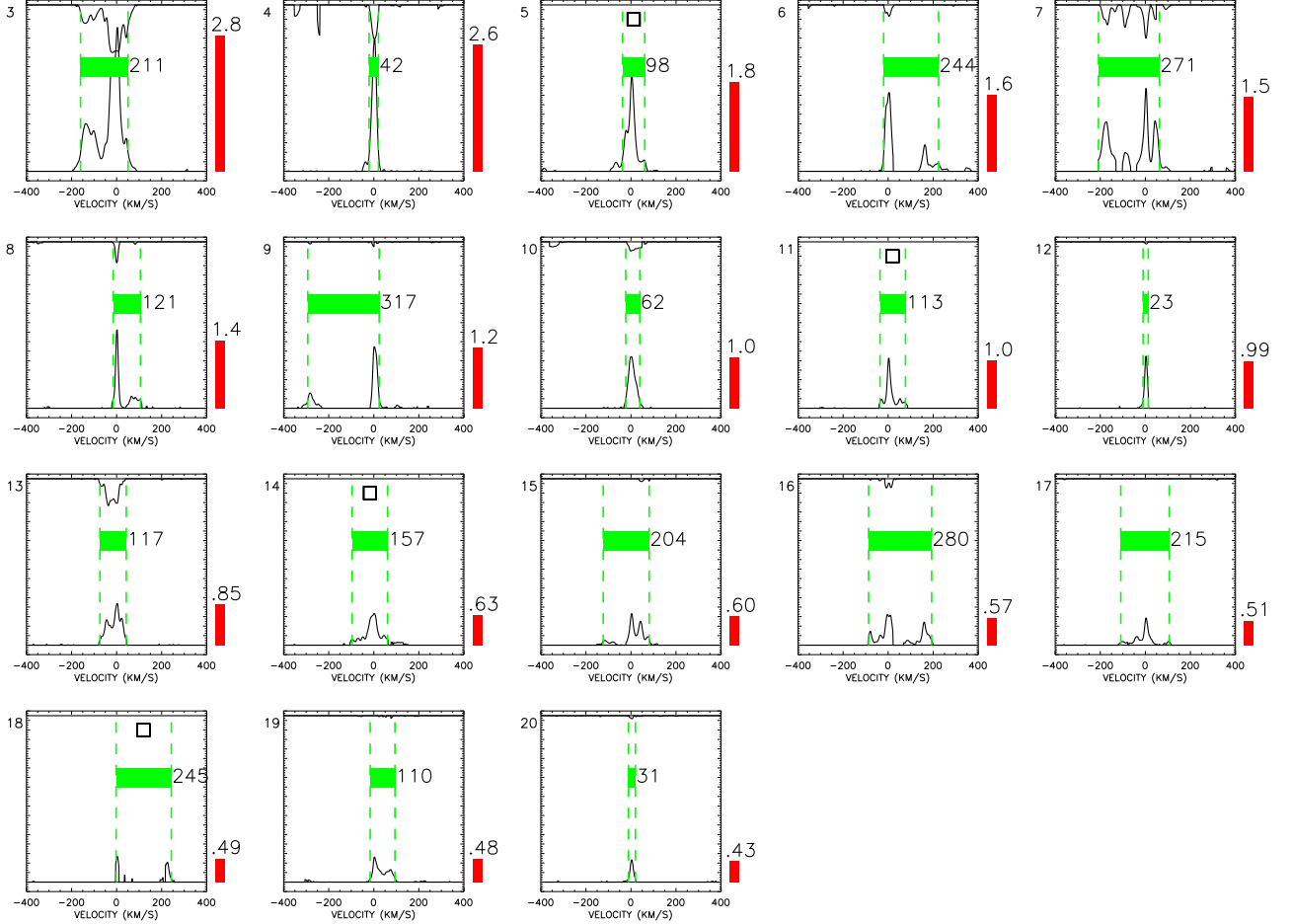


Fig. 2.— C IV systems from Table 1, with peak C IV optical depth above 0.4. Each thumbnail corresponds to one system from the Table, indexed by the small numeral in the upper left. The lower plot is C IV optical depth as a function of velocity, in  $\text{km s}^{-1}$ , for the automatically detected system, with zero velocity marking the position of peak optical depth. The upper curve is the corresponding Si IV flux, normalized to unity, with open squares marking systems where Si IV absorption is in the Ly  $\alpha$  forest. The horizontal green bar marks the automatically determined full width at tenth max of the system (with endpoints denoted by vertical dashed green lines); this width, in  $\text{km s}^{-1}$ , is marked to the right of the green bar. The vertical red bar denotes the peak C IV optical depth whose value is given above the bar.

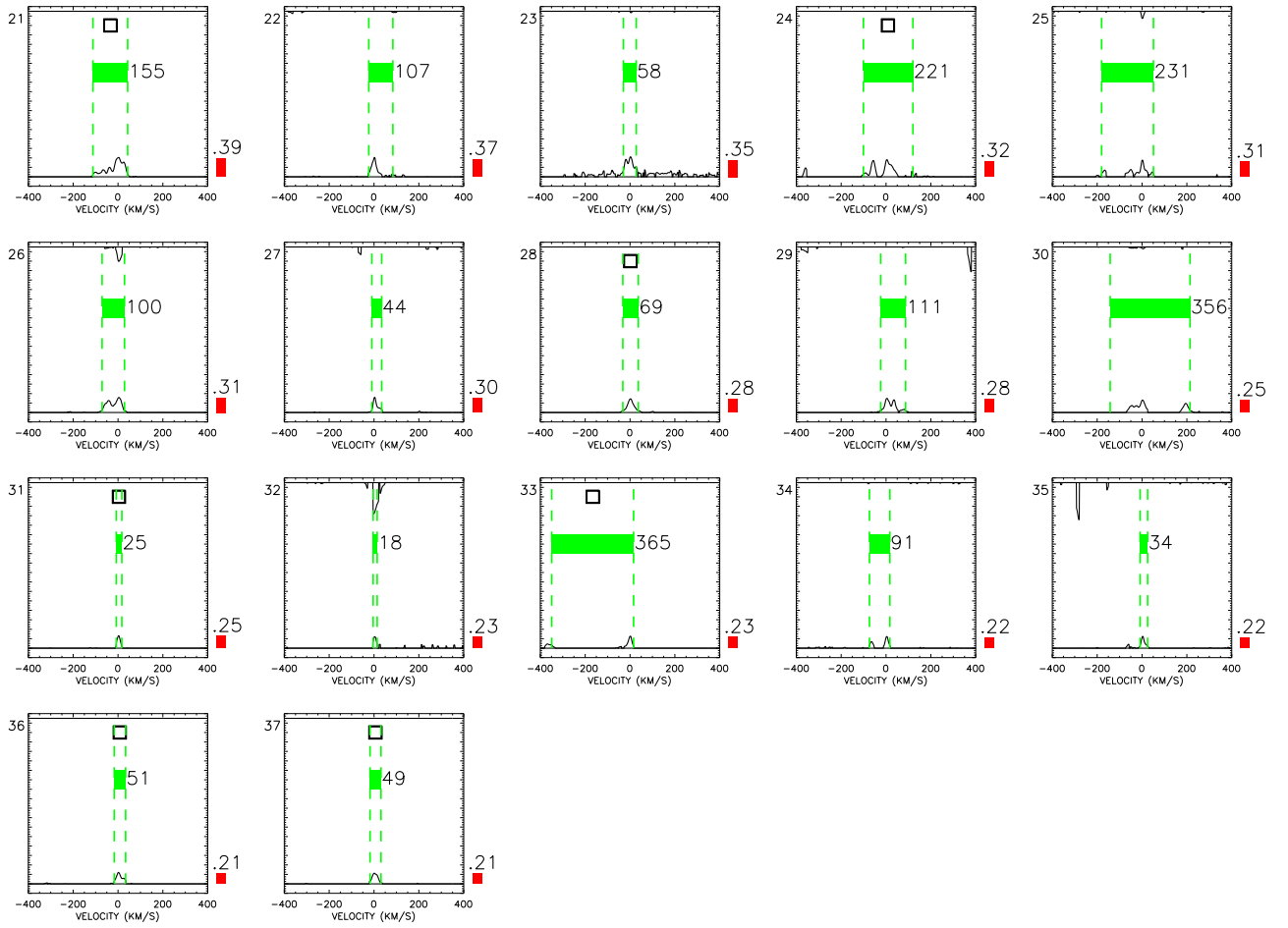


Fig. 3.— As in Fig. 2, for peak optical depth between 0.2 and 0.4.



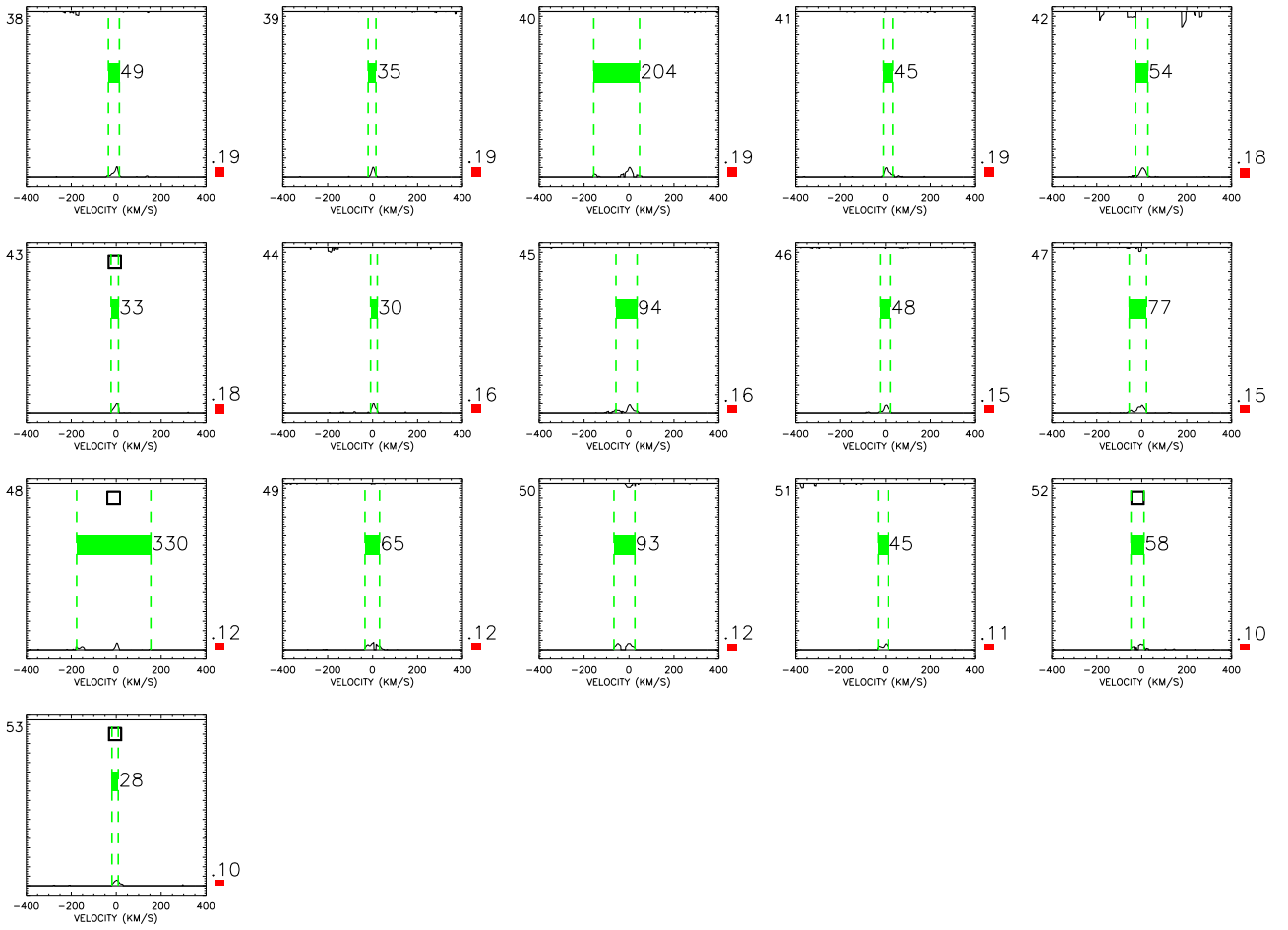


Fig. 4.— As in Fig. 2, for peak optical depth below 0.2.

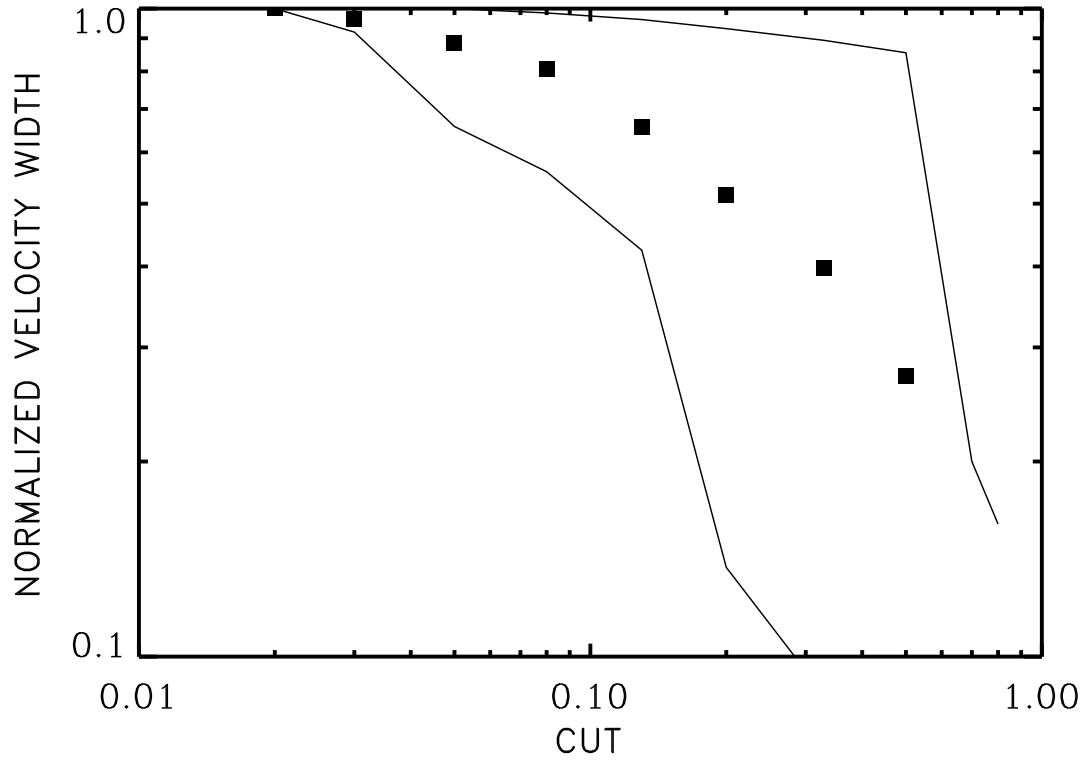


Fig. 5.— *Filled squares* : average ratio of the full width measured at the specified cut level relative to that measured at a cut of 0.02 for the 6 objects with  $1.4 < \tau < 3$ . *Solid lines* : maximum and minimum values measured in the sample.

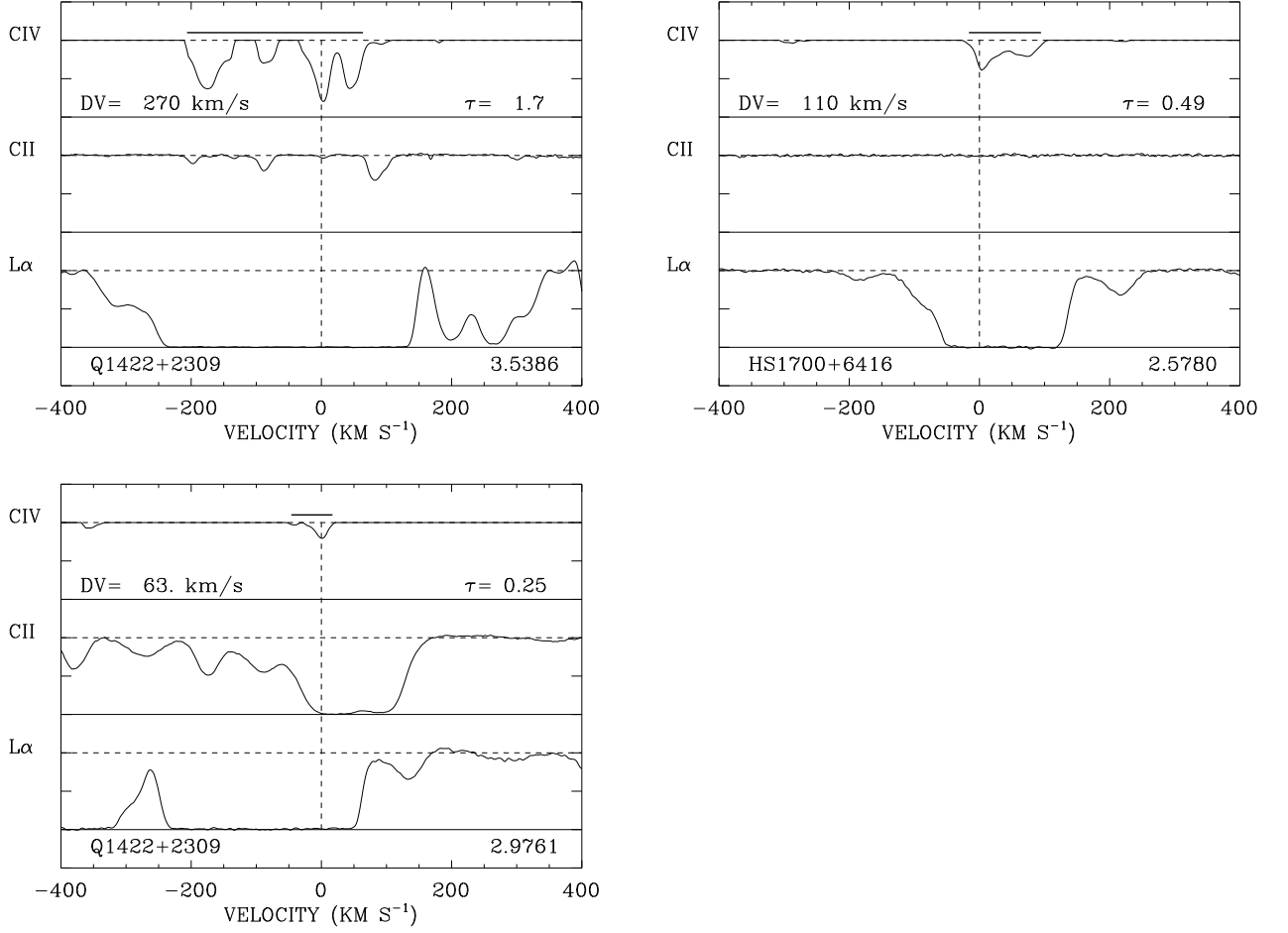


Fig. 6.— Sample plots showing the width at a tenth of the peak C IV optical depth for a range of  $\tau_p$ . The width is shown at the top of each plot over the C IV absorption (*solid horizontal line*). The *dashed vertical line* shows the position of the peak  $\tau$ . Absorption profiles for C II and Ly  $\alpha$  are also shown. Note that for the  $z = 2.9761$  system in Q1422+2309, C II is in the Ly  $\alpha$  forest.

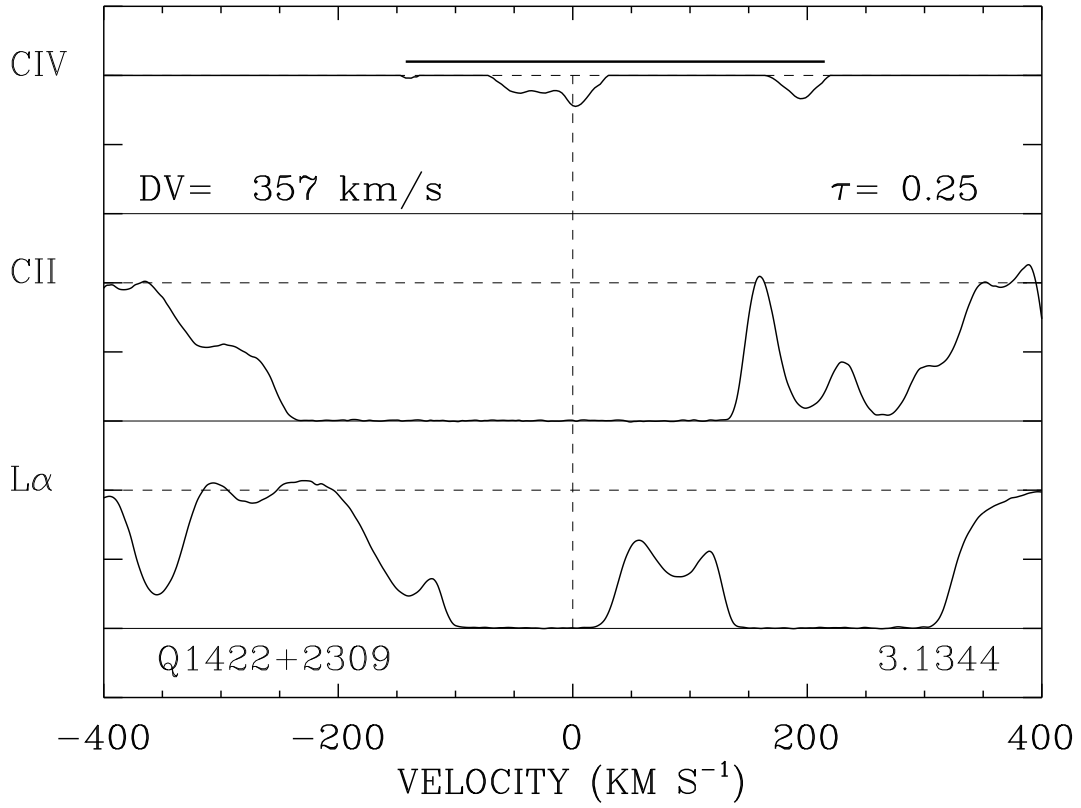


Fig. 7.— Sample plots showing an example where the method may have connected two neighboring systems and produced too large a velocity width. Note that C II is in the Ly $\alpha$  forest for this system.

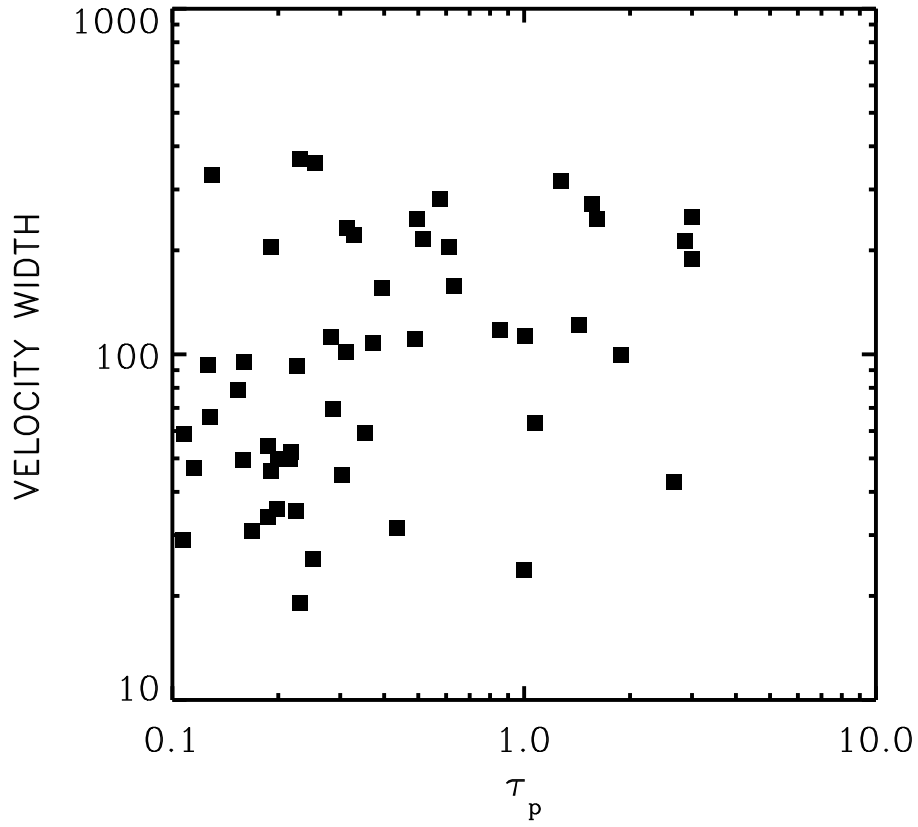


Fig. 8.— FWTM velocity width determined by the automatic procedure versus peak optical depth in C IV 1548Å.

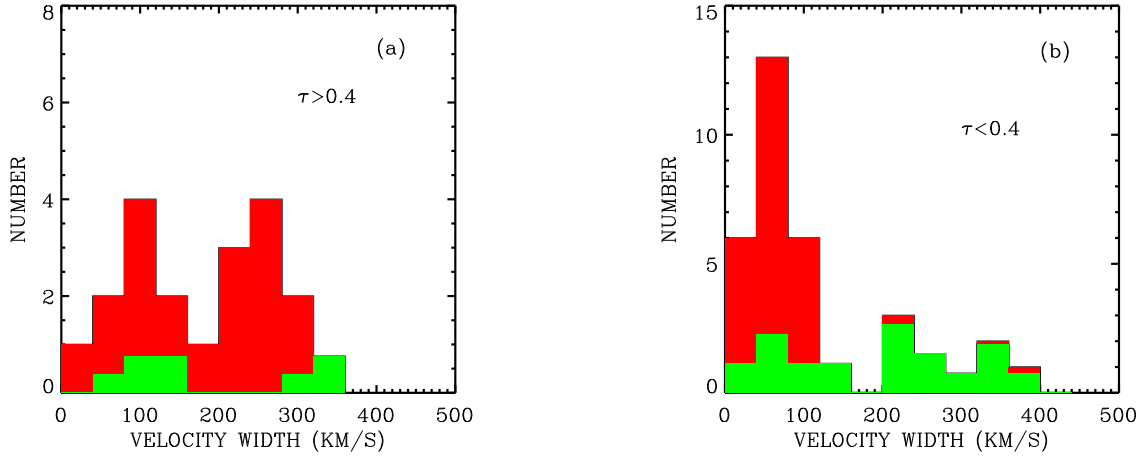


Fig. 9.— *Panel (a)* : histogram of the velocity widths for systems with  $\tau_p > 0.4$ . *Panel (b)* : histogram of the velocity widths for systems with  $\tau_p = 0.1 - 0.4$ . *Red (dark) histogram*: measured values; *green (light) histogram*: expected number of false systems.

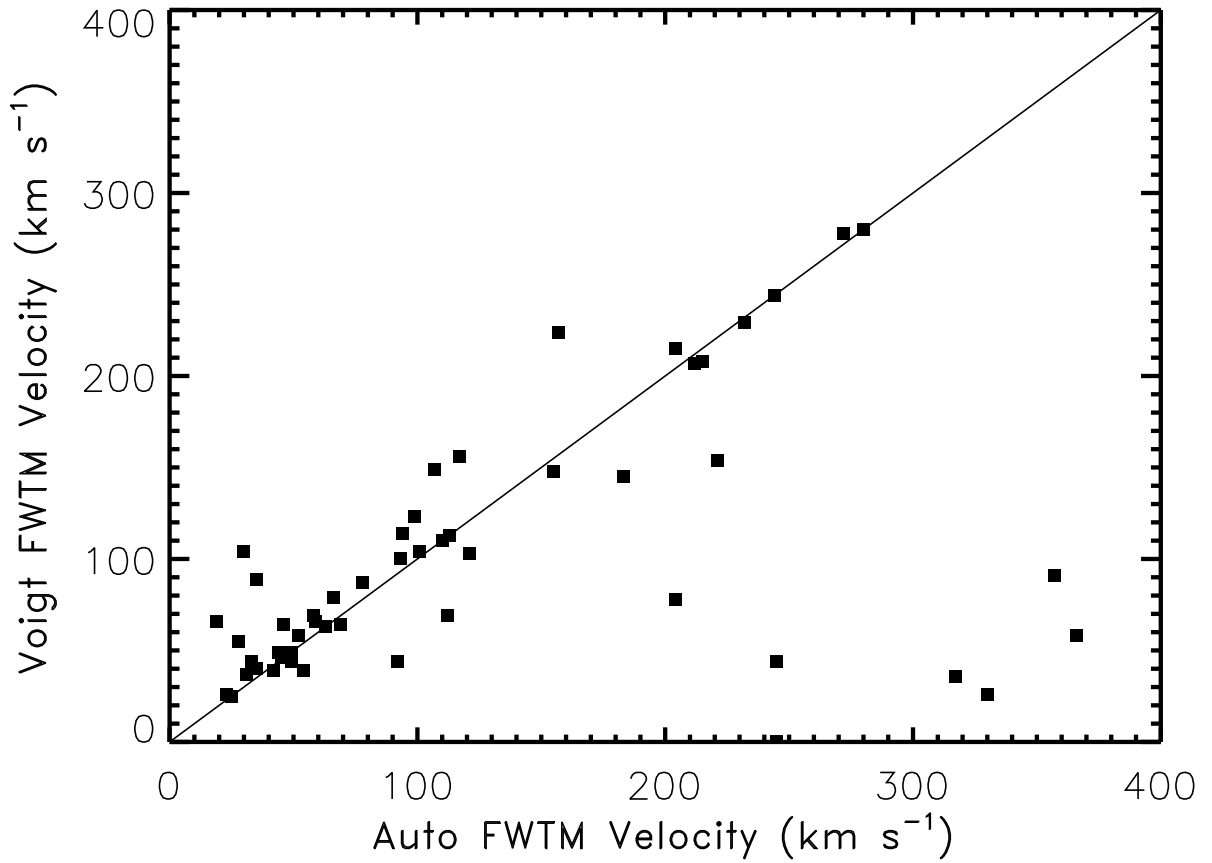


Fig. 10.— Comparison of the automated measure of FWTM with the same quantity measured from Voigt profile fits. The two measures generally agree well except for the small number of cases for which the Voigt profile fitting has treated a wide velocity system as two separate complexes.

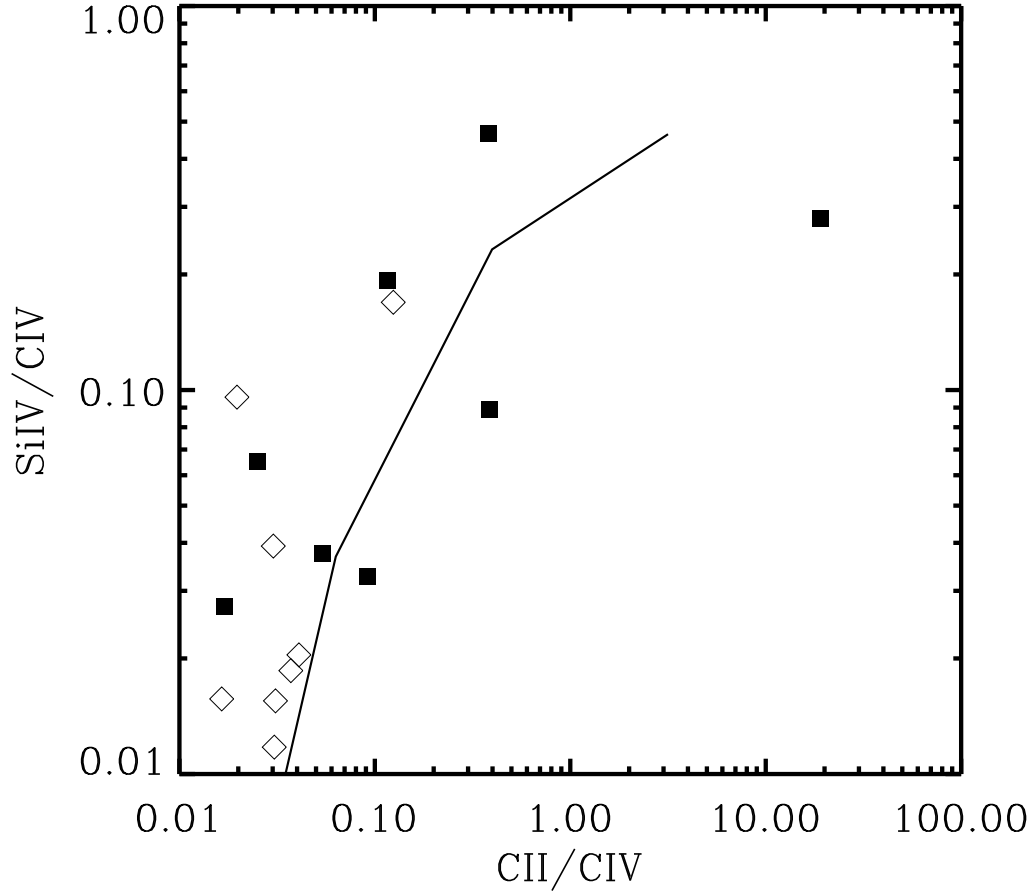


Fig. 11.— Si IV/C IV versus C II/C IV measured from Voigt profile fitting is compared to a simple prediction made using an AGN power law spectrum and computed for a Si/C ratio of 2.5 times solar. *Filled squares:* systems with  $\Delta v(\text{FWTM}) > 100 \text{ km s}^{-1}$ . *Open diamonds:* systems with  $\Delta v(\text{FWTM}) < 100 \text{ km s}^{-1}$ .



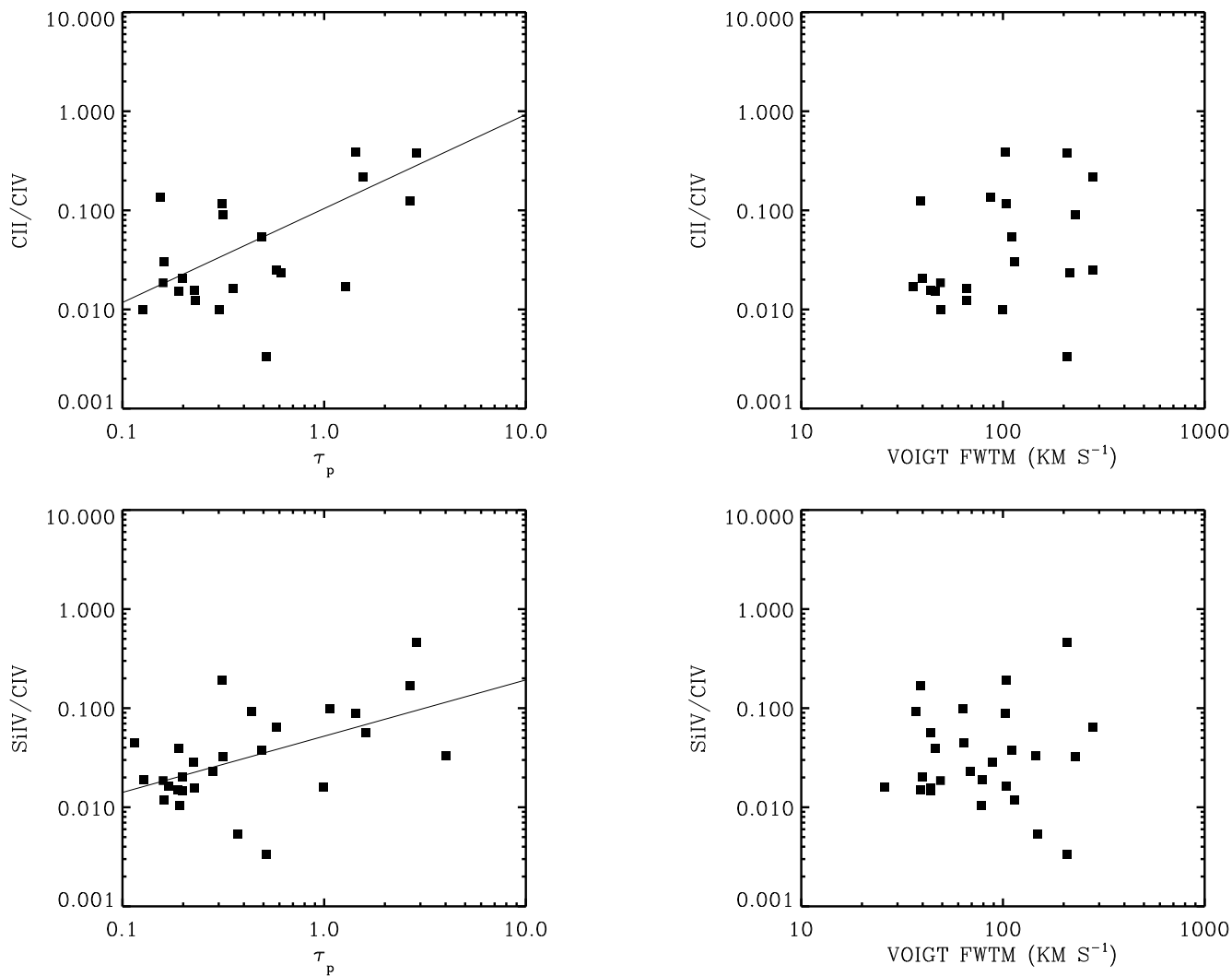


Fig. 12.— Ion ratios versus peak C IV 1548 optical depth and FWTM velocity width. *Solid lines*: simple power law fits to the dependence of the ion ratios on peak optical depth. C II/C IV shows a near-linear dependence on  $\tau_p$ , whereas Si IV/C IV shows a shallower rise.